Transient simulations of heavy-duty diesel engines with focus on the turbine

by

Niklas Winkler

April 2008
Technical Reports from
Royal Institute of Technology
KTH Internal Combustion Engines
SE - 100 44 Stockholm, Sweden

Akademisk avhandling som med tillstånd av Kungliga Tekniska Högskolan i Stockholm framlägges till offentlig granskning för avläggande av teknologie licentiatexamen den 9/4 2008 kl 10 i Sal M3, Brinellvägen 64, Kungliga Tekniska Högskolan, Valhallavägen 79, Stockholm.

Universitetsservice US–AB, Stockholm 2008

Abstract

The finite response time of the turbocharger is the most notable effect of transient operation on a turbocharged diesel engine. To fulfil future emission requirements high amounts of transient EGR will be required. This implies that advanced turbocharger systems have to be introduced to enable high boost pressures with improved or at least maintained response time. The increased amount of tunable parameters from the more advanced turbocharging system will make it difficult to optimise the engine experimentally. Therefore the wish is to optimise the engine numerically, however this is a difficult task which demands more knowledge within the field of modelling the gas exchange system and its components, which is the aim of the present work.

Engine simulations have been performed in the 1-dimensional fluid dynamic code GT-Power for transient operation and validated with engine measurements. The turbine was modelled according to the state of the art which is via look-up tables with measured turbine performance data from a steady-flow rig and used under the assumption that the turbine behaves in a quasi-steady manner. Turbine performance data was also obtained via the semi-empirical turbine design software, Rital for comparison. A heavy-duty diesel engine has been modelled with two different gas exchange system configurations. The standard configuration with a single twin-entry turbine and a rebuilt gas exchange system including a two-stage turbocharging system and high pressure loop for EGR.

The results shows that it is difficult to predict the performance of the gas exchange system and its components, especially the turbine performance. When trying to predict turbine performance under transient operation the difficulties added, compared to stationary operation are long scale transients as wall temperature gradients in the cylinder and the exhaust manifold which directly influences the amount of isentropic energy to the turbine. This makes it even more difficult to predict the isentropic exhaust gas energy content compared to stationary operation, which is difficult to measure and therefore to state how well the turbine model actually performs.

However, even though it is difficult to predict engine performance in detail the models have proved to be useful for concept studies as a help in engine design.

List of Papers

Paper 1

Instantaneous On-Engine Twin-Entry Turbine Efficiency Calculations on a Diesel Engine
SAE Technical Paper 2005-01-3887
Niklas Winkler, Hans-Erik Ångström and Ulf Olofsson.
Presented at 2005 SAE Powertrain & Fluid Systems Conference, San Antonio

Paper 2

Study of Measured and Model Based Generated Turbine Performance Maps within a 1D Model of a Heavy-Duty Diesel Engine Operated during Transient Conditions
SAE Technical Paper 2007-01-0491
Niklas Winkler and Hans-Erik Ångström.
Presented at 2007 SAE World Congress, Detroit

Paper 3

Simulations and Measurements of a Two-Stage Turbocharged Heavy-Duty Diesel Engine Including EGR in Transient Operation
SAE Technical Paper 2008-01-0539
Niklas Winkler and Hans-Erik Ångström.
Accepted for presentation at the 2008 SAE World Congress, Detroit

The author ran the experiments, evaluated the data, performed the simulations and wrote the papers supervised by HEÅ. UO contributed in the writing process and reviewed paper no. 1.

"The purpose of computing is insight not numbers"
Hamming's motto

Abbreviations, Symbols and Subscripts

Abbreviations

EGR	exhaust gas recirculation
ETC	European transient cycle
NO_x	nitrogen oxides
PM	particle matter
PR	pressure ratio
VGT	variable geometry turbine

Symbols

C	absolute velocity
E	energy
I	shaft moment of inertia
T	temperature
U	blade tip speed
W	relative velocity
c	specific heat
p	pressure
t	time
u	flow velocity
α	absolute flow angle
β	relatve flow angle
δ	deviation
γ	ratio of specific heats
ρ	density
ω	rotational speed
η	efficiency
τ	torque

Subscripts

0	stagnation
1, 2, 3	turbine internal locations
c	corrected
k	kinetic
b	blade
m	meridional
red	reduced
ts	total to static
T	turbine
C	compressor
TC	turbocharger
mech	mechanical
θ	tangential

Contents

Part I

Overview and Summary

CHAPTER 1

Introduction

For heavy-duty applications, i.e. road-going transport vehicles the diesel engine is today the only realistic option due to its high efficiency as compared to other alternatives. Even though engine development the past years has been focusing on reduction of emissions the road transportations are today the largest contributor to nitrogen oxides (NO_x) and the second largest contributor to particle matter (PM), see e.g. Laguna-Gomez (2007). The primary emission reduction mechanisms for NO_x is Exhaust Gas Recirculation (EGR) and PM by development of the injection system and increasing injection pressure. As higher rates of cooled EGR are introduced higher boost levels are needed to maintain the oxygen content.

The purpose of turbocharging has in the past been to increase the power to weight ratio of the engine. By increasing the amount of air available for the combustion process more fuel can be burned effectively. Today, the primary goal to use turbocharging for heavy-duty applications is still to raise the power to weight ratio, but it is more and more used as a help to optimize the engine to obtain lower emissions in order to manage future emission legislations while maintaining or even improving fuel efficiency.

The turbocharger itself has become a mature product. Improvements on the turbomachine will therefore be rather incremental. Therefore, the focus for development has turned more towards the turbocharger application. New complex systems to improve exhaust energy utilisation over a wide engine operating range will be more frequently incorporated into the engine design such as Variable Geometry Turbines (VGT), multi-stage turbocharging, turbo compounding or various mechanically additional driven compressors.

1.1. Motivation

The main challenge for engine manufacturers is to be able to follow the transients in the transient emission certification cycles as the European Transient Cycle (ETC) without exceeding the emission limits and to maintain or improve fuel efficiency. For turbocharged diesel engine operation the most notable effect of transient response is turbocharger lag due to the finite response time of the turbocharger, which is caused by the lack of a mechanical connection between the turbocharger compressor and the crank-shaft. The change in energy delivered by the engine to the turbine must first accelerate the turbocharger shaft assembly to make it possible for the compressor to produce boost pressure.

To fulfil future emission requirements high amounts of transient EGR will most likely be needed. This implies that advanced turbocharger systems have to be introduced to enable high boost pressure with improved or at least maintained response time.

Thus the turbocharger system is more and more in focus for overall engine performance. With the more complex turbocharging systems the amount of tunable parameters increases which makes it difficult to optimise the engine experimentally. Therefore the wish is to optimise the engine numerically, however this is a difficult task which demands more knowledge within the field of modelling the gas exchange system and its components.

The main aim of the project is to develop new modelling tools to better predict engine performance during transient operation than the tools used today. The first part of this project, which is presented, aims at gaining more knowledge of turbocharger and complex turbocharger system performance on engine and the simulation possibilities of such engines in transient operation. The commercial simulation code GT-Power from Gamma Technologies (2004) has been used for engine simulations. As a complement to turbine modelling via measured turbine performance maps the turbine modelling tool, Rital from Concepts NREC (2005) was used. Measured data for model validation was obtained from a heavy-duty diesel engine equipped with a single radial twin-entry turbine and a complex two-stage turbocharger system in series including short route EGR installed and run in a test cell at KTH.

CHAPTER 2

Turbocharging the Diesel Engine

2.1. General Principals

The typical turbocharger in an automotive application is a simple device, which is mechanically separated from the reciprocating internal combustion engine. The turbocharger consists of a centrifugal compressor which is mechanically connected to and driven by a single radial turbine. The turbine extracts energy from the otherwise wasted exhaust gases. The role of the compressor is to increase the air density entering the combustion chamber, thus a higher available mass of air is achieved for the combustion process, figure 2.1.

Even though the turbocharger itself is a simple device the design process is complex due to the unsteady environment when employed on a reciprocating internal combustion engine. The engine exhausts are characterised by short and long scale transients, the former driven by exhaust valve events and the latter by engine operating conditions. The complexity comes from that the long scale transients makes the turbocharger work in a wide range and the short scale transients through complicated turbocharger performance analysis.

How well a turbocharger works on a given engine can be measured as turbocharger efficiency (η_{TC}), which is the product of compressor (η_C) and

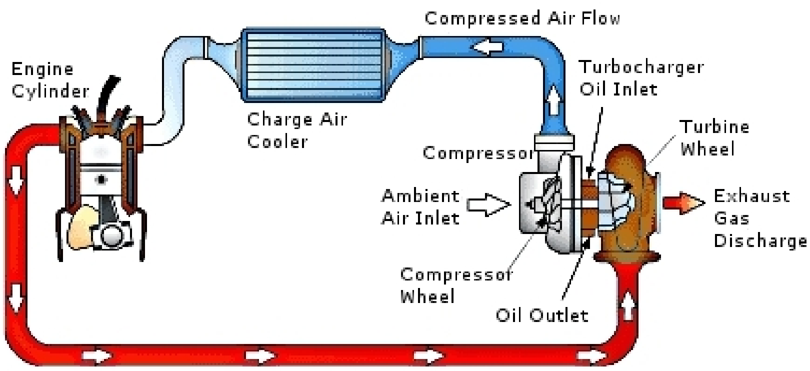

FIGURE 2.1. Schematic of an engine turbocharger system, from *Garrett*.

turbine efficiencies (η_T) including losses in the drive system (η_{mech}) of the connecting shaft according to equation 2.1,

$$\eta_{TC} = \eta_C \eta_T \eta_{mech} \quad (2.1)$$

where the isentropic efficiency of the turbine is defined as the ratio of the actual work output to the isentropic work input and the isentropic efficiency of the compressor as the ratio of the ideal work input, assuming that the compression process is isentropic, to the actual work input.

The presence of a turbine in the engine exhaust system increases the engine back pressure. High turbocharger efficiency will give a pressure rise exceeding the increased back pressure that will decrease pumping losses, which will directly improve engine efficiency.

2.2. Turbocharging System

Figure 2.2 shows the idealised engine cycle for a constant pressure combustion engine and the energy available for the turbine. Ideally there are two main methods to extract the exhaust energy, the constant pressure and the pulse pressure system.

In a constant pressure system the exhaust manifold includes a large enough volume to dampen out the pulsations from the engine. The theoretically available energy for this type of system is shown by the p-V diagram bounded by the points 7-8-10-11, figure 2.2.

In the pulse pressure system an attempt is made to extract energy associated with the high pressure pulsations from the opening of the exhaust valve including the energy available for constant pressure turbocharging. To preserve the kinetic energy of the exhausts an exhaust manifold which is as short and narrow as possible is used. Ideally, the available energy for this type of system is shown by the p-V diagram bounded by the points 5-8-10-11-13, figure 2.2.

The pulse pressure system makes more exhaust gas energy available for the turbine than the constant pressure system, but with a pulse pressure system it is more demanding to achieve a high mean turbocharger efficiency over the engine cycle. The unsteady flow makes the turbine work in off-design for some parts of the cycle, see e.g. Watson & Janota (1982), and it is more challenging to analyse the turbine performance. For automotive applications pulse pressure turbocharging is used since it has shown higher potential with respect to exhaust gas energy utilization.

2.3. Matching the Turbocharger and Engine

Due to the different flow characteristics of the reciprocating internal combustion engine and the rotordynamic machine devices, i.e. the turbine and compressor matching a turbocharger to an engine is a difficult task. The internal combustion engine works like a positive displacement pump where its volumetric flow

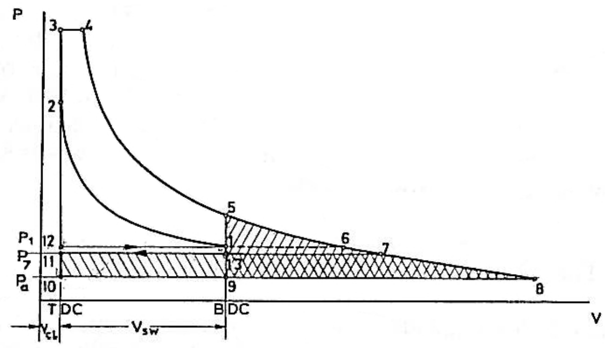

FIGURE 2.2. Ideal constant pressure cycle, Watson & Janota (1982)

rate increases close to linearly with engine speed. The operational range for a heavy-duty diesel engine is from 600 to above 2000 rpm while smaller engines can work in an even broader operational range. The desire is to obtain high inlet air density over the entire range so an engine of smaller size can be used without sacrificing power output.

The turbine has similar characteristics as a nozzle, i.e. the pressure ratio across the turbine is proportional to the density and the square of the flow velocity, $\Delta P \propto \rho u^2$. Thus the limitations for a turbine is that at low engine speeds, i.e. low mass flow rates, the expansion ratio across the turbine is small and hence the power output. At high flow rates the turbine reaches a flow limit where it becomes choked, i.e. the velocity within any part of the volute or rotor becomes sonic, thus the pressure upstream the turbine rises without an increase in mass flow rate. Figure 2.3a shows the flow characteristics of a radial turbine.

The volumetric flow rate through the compressor is controlled by the inlet area and the velocity of the flow into the impeller. The rotational speed of the impeller controls the tangential velocity of the flow, thus the power input which is limited by the maximum speed of the compressor due to limitations of impeller material properties. Since the rotational speed does not directly influence the flow velocity onto the impeller its operating flow range is relatively narrow, figure 2.3b. As shown by Baines (2005) the flow range for a centrifugal compressor is exponentially decreasing with the pressure ratio, which is limited by surge and choke. Surge can occur at low flow velocities into the impeller due to flow separation at the impeller blades and at high flow rates the velocities within the impeller may become sonic and choke will occur.

A general limitation of the turbocharger in an automotive application is its transient response, i.e. to follow the load changes of the engine. The time it takes to reach a certain turbocharger speed and produce boost is caused

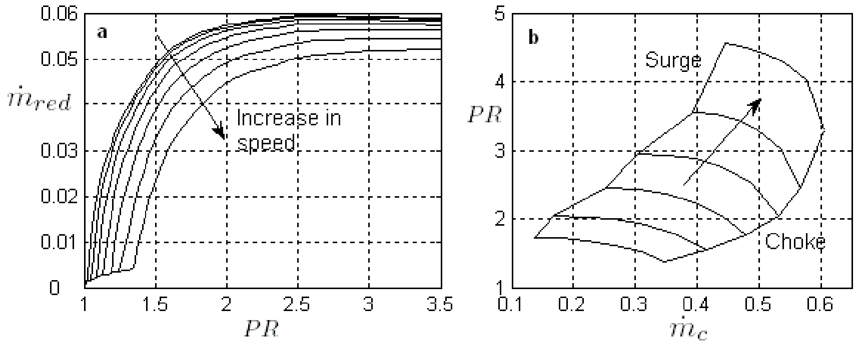

FIGURE 2.3. Flow characteristics for a radial turbine, a) and a centrifugal compressor, b). Each speed line corresponds to a constant rotational speed, PR denotes pressure ratio and the mass flow rates are given as corrected and reduced, discussed in chap. 4.2.

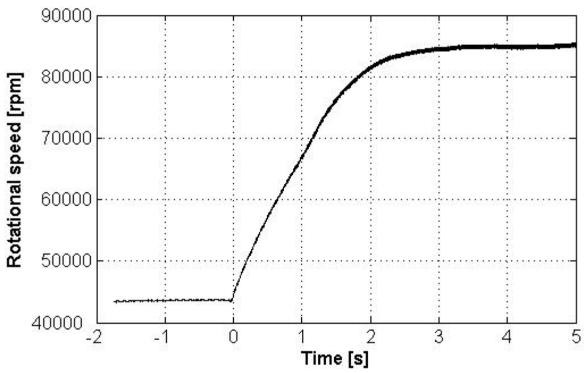

FIGURE 2.4. Turbocharger speed on an engine during a load transient, i.e. load step demand at constant engine speed.

by the lack of a mechanical connection between the turbocharger compressor and the crank-shaft. The energy delivered to the turbine must first accelerate the turbocharger shaft assembly to make it possible for the compressor to produce boost pressure. The time it takes for the turbocharger to spin up is called turbocharger lag. Figure 2.4 shows a typical example of the spin up process of a turbocharger for an instant load step demand. To improve its transient response and low speed performance a smaller turbocharger can be used, but it will become choked for high engine speeds. On the other hand a large turbocharger will give good performance at high engine speeds but due to its high inertia and the higher flow rate needed for the same boost pressure it will give poor transient response and low speed performance. At too low engine speeds the exhaust flow will not be sufficient for the turbocharger to produce boost pressure, i.e. there is a boost threshold speed, which should not be confused with turbocharger lag. A way to improve these problems is to use variable geometry turbines and/or multi-stage turbocharging, which have in many ways improved the turbocharger to engine matching possibilities.

2.3.1. *Variable Geometry Turbine, VGT*

The VGT is considered as an effective approach to the turbocharger to engine matching problem. By varying the inlet turbine geometry it is similar as having a finite range of turbine sizes in one unit. At low engine speeds the VGT is kept closed to raise the pressure upstream the turbine, thus the isentropic energy from the exhausts raises. At high engine speeds the inlet area is increased to avoid overboosting and high engine back pressure.

The inlet area is mainly adjusted in two ways, by a sliding nozzle ring mechanism, figure 2.5 or by pivoting nozzle blades, figure 2.6. The sliding nozzle ring mechanism keeps the nozzle blades fixed and changes the inlet area due to an axial movement of the sliding wall. By pivoting the nozzle blades the area between the blades changes as well as the vane angle.

2.3.2. *Two-stage Turbocharging*

Two-stage turbocharging is an effective way of overcoming the limitations on boost pressure imposed by current compressor materials, to maintain its operational range and to improve transient response.

The temperature downstream the compressor (T_{02}) can be derived from the pressure ratio, i.e. static outlet (P_2) and total inlet pressure (P_{01}), and inlet total temperature (T_{01}) including the compressor efficiency, which is defined as the ratio between isentropic work if the gas is ideally compressed and actual work needed for the compression,

$$T_{02} = T_{01}\left(\frac{(P_2/P_{01})^{(\gamma-1)/\gamma}}{\eta_{C,ts}} + 1\right) \tag{2.2}$$

Already for a boost pressure of 1.5 bar and an assumed compressor efficiency of 70% the outlet temperature is 150^0C at an inlet temperature of 25^oC. At these temperatures the compressor impeller materials needs to be more exotic than the normally used aluminium alloys, since its material properties starts to decrease significantly.

In a two-stage turbocharging system an intercooler can be used between the compressor stages which reduces inlet air temperature to the high pressure stage, thus it is possible to reach higher boost pressures with the standard

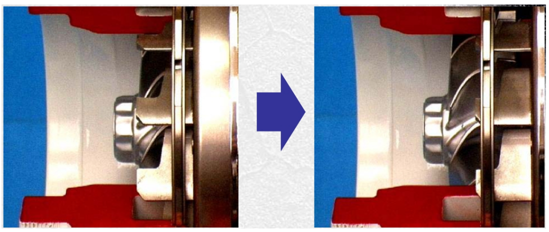

FIGURE 2.5. VGT with a sliding nozzle ring mechanism, closed and open position respectively, from *Cummins Turbo Technologies*.

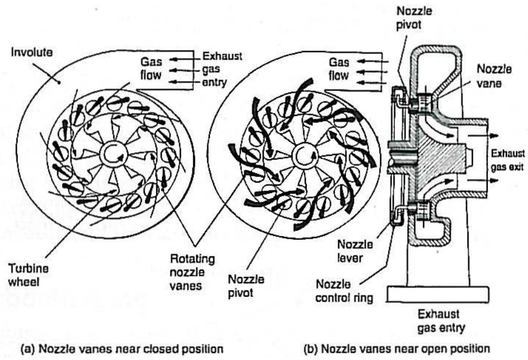

FIGURE 2.6. VGT with variable nozzle blades, from Heizler (1995)

impeller material. Increased air density also implies that a smaller compressor can be used and that less power is needed to reach the desired pressure raise.

In a sequential turbocharger arrangement two or several different sized turbochargers can be used where the flow can be switched so that the best suited turbocharger for that operational point is used. Sequential turbocharging can improve low end torque, response time and/or operational range.

2.4. The Turbomachine

Ideally the turbomachine works with the principal described by the Euler turbomachine equation, i.e. when no work transfer occurs in the volute and heat transfer is negligible. The Euler equation is derived from Newton's second law of motion applied to a rotating system. The generated torque (τ) is the change in angular momentum, i.e. the change in the product of the radius (r) and tangential velocity (C_θ). Thus the work transfer, i.e. rate of kinetic energy change per unit mass flow, ($\Delta E_{k,x}$), which is the torque times the angular velocity (ω) is,

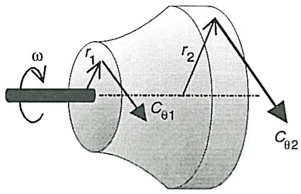

FIGURE 2.7. Swirl in a turbomachine rotor from Japikse & Baines (1997).

$$\Delta E_{k,x} = \tau\omega/\dot{m} = \omega\left(r_1 C_{\theta 1} - r_2 C_{\theta 2}\right) = \left(h_{0,1} - h_{0,2}\right) \tag{2.3}$$

where $(\dot{m})$ is the mass flow rate. The work per unit mass flow, which is equal to the change in total enthalpy, (h_0) of an adiabatic process is thus proportional to the temperature change over the turbomachine.

2.4.1. *The radial turbine*

The radial turbine consists of a volute casing, a set of vanes which are sometimes omitted, the turbine housing and the turbine rotor. The purpose of the volute is to expand the tangentially incoming flow to a high flow velocity and to distribute the flow circumferentially to achieve a uniform mass flow and static pressure at the volute exit. The vanes (if present) then further accelerate the flow reducing pressure, increasing kinetic energy and turn the flow to the designed angle. In the rotor the incoming flow is expanded through the rotor passages and the kinetic energy is extracted and transferred to mechanical energy.

Expanding the Euler equation according to the gas velocity components at the rotor inlet and the rotor exit, notations according to figure 2.8, gives design criteria for the rotor and volute,

$$\Delta E_{k,x} = \frac{1}{2}\left[\left(U_2^2 - U_3^2\right) - \left(W_2^2 - W_3^2\right) + \left(C_2^2 - C_3^2\right)\right] \tag{2.4}$$

where (W) denotes the flow velocity relative to the rotor, (C) the absolute flow velocity and (U) the blade tip speed. In a radial turbine the change in inlet and exit radius gives a change in blade speed such as $U_2^2 > U_3^2$. The second term which relates inlet and exit relative flow velocities shows that acceleration of the flow within the rotor passages is desired. To maximise the third term a high inlet absolute flow velocity from the volute and a minimum rotor exit absolute flow velocity is desired since the kinetic energy of the flow will be dissipated. According to Japikse & Baines (1997) there does not exist any analytical way to select an exit radius of the rotor to optimise the energy transfer, only conventions.

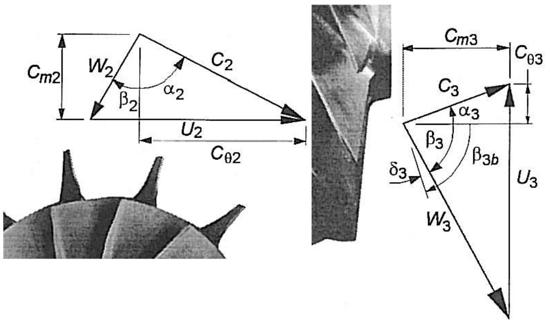

FIGURE 2.8. Velocity relations at the rotor inlet, left and exit, right.

The ratio of expansion between the volute and the rotor is denoted as reaction (Λ) and defined as the enthalpy change, (Δh_0) in the rotor and the total enthalpy change across the stage, i.e. from volute inlet to the rotor exit,

$$\Lambda = \frac{\Delta h_{rotor}}{\Delta h_{0,stage}} \tag{2.5}$$

For an isentropic radial inflow turbine with complete exhaust energy recovery and a reaction of 50%, which is common design practice, maximum efficiency occurs ideally at a blade speed ratio of $1/\sqrt{2}$, Watson & Janota (1982), i.e. the ratio between the rotor inlet blade tip speed (U_2) and the gas velocity isentropic expansion (C_s) across the stage,

$$\frac{U_2}{C_s} = \frac{r\,(2\pi N/60)}{\sqrt{2c_p T_{0,0}\left[1-\left(\frac{p_3}{p_{0,0}}\right)^{(\gamma-1)/\gamma}\right]}} \tag{2.6}$$

where index $(0,0)$ denotes the total turbine inlet state and (N) rotational speed. Figure 2.9 shows measured efficiency for a nozzleless radial turbine as a function of the blade speed ratio for different constant rotational speeds. The left part of the efficiency parabola relates to high gas velocities and the right to lower gas velocities.

The angle at which the flow approaches the rotor (β_2) relative to the inlet blade angle (β_{2b}), i.e. the incidence angle (i), equation 2.7 has a significant effect on the efficiency of the rotor. At a non optimal inlet incidence angle work has to be put in to turn the flow according to the blade passages.

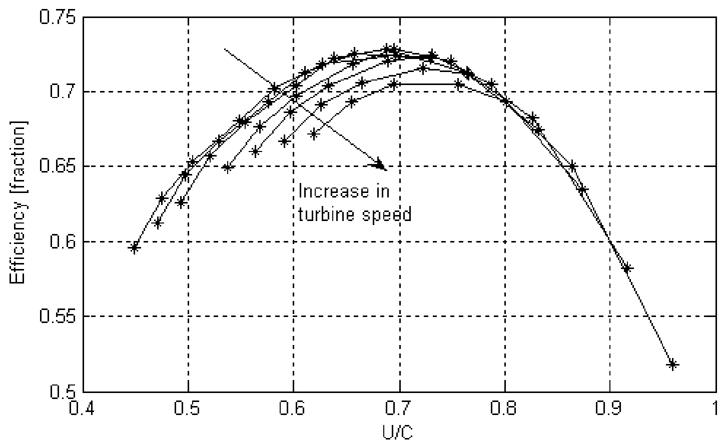

FIGURE 2.9. Measured turbine efficiency as a function of blade speed ratio at constant rotational speeds.

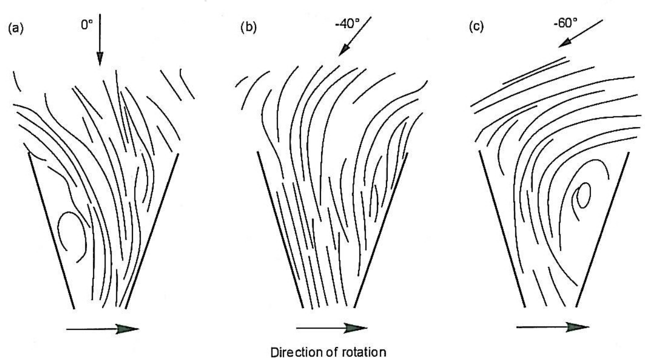

FIGURE 2.10. Observed flow behaviour in a radial turbine rotor at different incidence angles, measurements performed by Wooley and Hatton 1973, from Baines (2003)

$$i = \beta_2 - \beta_{2b} \tag{2.7}$$

A flow visualization is shown in figure 2.10 where the flow is approaching a rotor at different incidence angles. The visualisation shows that a uniform flow without recirculation occurs for a somewhat negative incidence angle. This is due to that the radius diminishes more rapidly than the tangential velocity which causes a circulation of the flow to the pressure side where it stagnates, thus the flow will first approach the suction side and then the pressure side.

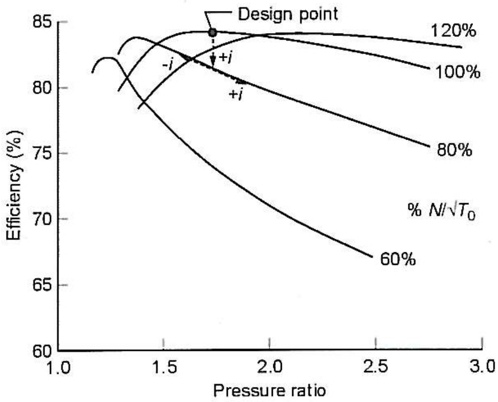

FIGURE 2.11. Off design characteristics for a radial turbine, figure from Baines (2003)

At incidence angles away from the optimal angle the flow will separate at the suction respectively at the pressure side.

The incidence angle changes with rotational speed and/or pressure ratio across the stage. Figure 2.8 together with equation 2.7 shows that changes in rotor speed, which are directly related to blade tip speed and pressure ratio, which influences the absolute gas velocity will affect the incidence angle. An increase in rotational speed will give a negative change in incidence angle and the opposite for a decrease in speed. An increase in pressure ratio will give a positive change to the incidence angle and vice versa for a decrease in pressure ratio. Figure 2.11 shows how changes in incidence angle changes the turbine performance. From the design point at maximum efficiency the performance is more affected to a decrease than in an increase in rotational speed, thus to positive changes in incidence angle. Performance changes can also be seen for changes in pressure ratio at the constant speed lines. Baines (2003) states that an optimal incidence angle can be found in the region of -20 to -40^o. Occasionally Yeo & Baines (1990) measured the incidence angle for a turbine at its maximum efficiency point, which showed that optimum incidence angle is close to -30^o.

Apart from incidence losses there are passage losses within the turbine. Passage losses include losses due to secondary flows, blockage and loss of kinetic energy due to growth of boundary layers in the volute and the rotor passages to the rotor throat. From the rotor throat to the space downstream the trailing edge there are losses due to the velocity field distribution downstream of the rotor. The trailing edge losses are influenced by the rotor exit deviation angle (δ), i.e. the difference between the exit blade angle (β_{3b}) and the exit flow angle (β_3), notations according to figure 2.8,

$$\delta = \beta_{3b} - \beta_3 \tag{2.8}$$

As previously pointed out from the expanded Euler equation, equation 2.4 a low absolute flow velocity is desired at the rotor exit and a large flow velocity relative to the blade angle, which is a contradiction. The velocity triangle for the rotor exit shows that the relative flow angle, thus the deviation angle is related to the blade tip speed and the tangential and the meridional component of the absolute velocity (C_{theta}) and (C_m). Unfortunately, there is not much data published on the deviation angle at the optimum design point. Baines (2003) summarised a few measurements where it can be seen that the deviation angle deviates from -7 to +2 degrees at the optimum design point. Baines & Yeo (1991) measured the absolute flow angle at the design conditions and at lower blade speed ratios. The measurements showed that the absolute flow angle was nearly constant across the rotor exit at the design point but deviates significantly at lower blade speed ratios due to that the flow velocity became higher near the rotor hub. For the twin-entry turbine used the exit absolute flow angle was not affected by different partial admission conditions.

2.4.2. *Centrifugal Compressor*

The air enters the centrifugal compressor from the axial direction and is diffused through the impeller and turned towards the radial direction. The flow leaves the impeller with substantial amount of kinetic energy. The flow then enters a diffuser where as much as possible of the kinetic energy is recovered. To collect the air and direct it to the inlet manifold a volute is used where additional diffusion occurs.

CHAPTER 3

State of the Art - Research

Turbocharging dates back to the time when the internal combustion engine was first developed. *Gottlieb Daimler* and *Rudolf Diesel* thought of increasing their engines performances by precompressing the available air for combustion. The first successful application of a turbocharger to compress the air was in 1925, by *Dr. Alfred Büchi* who achieved an engine power increase of 40%. For heavy-duty applications Scania, Cummins and Volvo started to experiment with turbochargers in the early 1950's. The first truck diesel engine equipped with a turbocharger was on the market in 1954.

Traditionally turbocharging has been associated with high power improvements but suffered from problems as reliability and turbocharger lag. Continuous development and new techniques have solved some of the past problems. Today, especially for road transport applications, turbocharging is more and more becoming a help to optimise engines for improved fuel efficiency and reducing harmful emissions.

3.1. Turbine performance under pulsating flow conditions

A significant amount of work have been performed in the field of radial turbine performance under unsteady flow conditions to asses the behaviour of the turbine in engine like conditions. The studies have primarily been performed in pulsating flow rigs to simplify the study of the turbine performance and to be able to use less advanced measurement apparatus than needed on an engine.

The first investigation of pulsating flow performance of radial turbines was conducted by Wallace & Blair (1965). The research was limited to that only the static pressure could be measured instantaneously. They found strong indications that the unsteady behaviour of the turbine is more apparent as the pulse frequency increases.

Dale & Watson (1986) presented the first turbine performance measurements under unsteady flow conditions with a complete set of instantaneous measured parameters. The measurements were conducted on a cold flow rig with a mean total inlet air temperature of 400K. The parameters measured instantaneously were mass flow rate air measured with hot-wire anemometers, static pressures with strain gauge pressure transducers and instantaneous turbine torque,τ as a sum of the mean and fluctuating torque, equation 3.1,

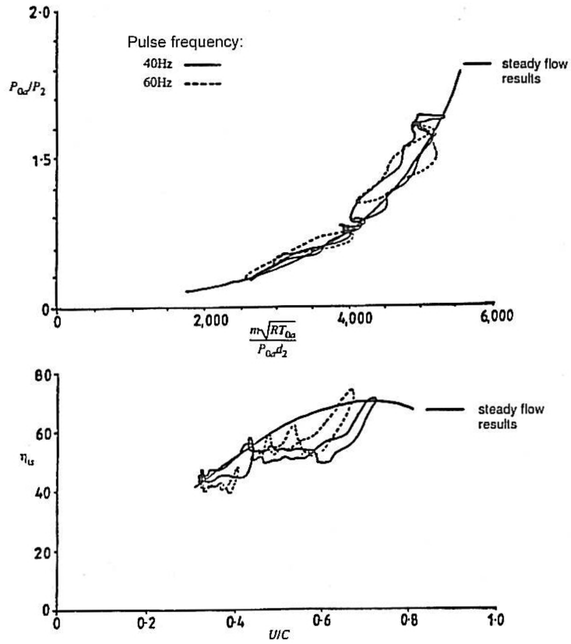

FIGURE 3.1. Efficiency versus velocity ratio, left and pressure ratio versus mass flow rate, right for unsteady and steady flow performance, from Dale (1990)

$$\tau = \overline{\tau} + I\frac{d\omega}{dt} \tag{3.1}$$

The mean torque ($\overline{\tau}$) was measured with a dynamometer and the fluctuating part of the torque was measured via the change in instantaneous turbine shaft speed ($d\omega/dt$) and the shaft moment of inertia (I). The speed was measured via a crystal clock with a frequency of 50MHz trigged by six positional datums every shaft revolution. These measurement techniques have been used by several researchers and are still used today Rajoo (2007). Dale & Watson (1986) and later Dale (1990) showed that instantaneous mass flow rate and efficiency under unsteady conditions deviates from that measured under steady flow conditions at the same pressure ratio. The mean mass flow rate as a function of pressure ratio is close to the steady-flow mass flow rate while the dynamic efficiency is below the steady-flow line which is shown with respect to the velocity ratio, figure 3.1.

Capobianco et al. (1989) used a small size automotive turbocharger to measure the power output from the turbine under pulsating flow conditions.

The result was that the swallowing capacity was approximately 5% higher than measured under steady flow, but the efficiency was significantly higher, 15-20%. As commented by Baines et al. (1994) this could imply that the energy in unsteady flow conditions is higher than under steady flow and not necessarily that the turbine efficiency is higher for unsteady operation. The proof that a pulse pressure wave contains more isentropic work than a steady flow one with the same cycle mean pressure was shown by Chen et al. (1996).

A major difficulty to derive the turbine performance from experimental data is the time difference between the measured isentropic conditions upstream the turbine and the actual turbine work output measured at the shaft. The flow approaches the rotor at different azimuthal angles around the volute, which makes it difficult to find a fixed parameter to compensate for the time difference. Researchers have used different phase shifting techniques to correlate these measures. The assumptions have been that the flow hits the rotor at a single point and that the fluid travels by the bulk and/or sonic velocity to derive the time difference from the measurement locations. Dale & Watson (1986) used the sonic velocity method while Winterbone et al. (1991) and Baines et al. (1994) used the bulk flow method for phase shifting. Arcoumanis et al. (1999) derived instantaneous efficiency for a mixed-flow turbine, which shows a similar behaviour as the radial turbine, with the two different methods for phase shifting used. Results showed that the method used for phase shifting gives a significant effect on the derived instantaneous efficiency.

Ehrlich (1998) performed extensive measurements on a 6-cylinder medium size diesel engine to analyse the on engine turbine performance, i.e. for pulsating flow including temperature fluctuations. Pressures were instantaneously measured before and after the turbine with strain gauge pressure transducers, temperatures with frequency response compensated fine wire thermocouples and flow velocities via Particle Image Velocimetry, PIV to derive the instantaneous mass flow rate. The measurements showed that the flow velocity, pressure and temperature within the volume of the exhaust manifold and turbine propagates with different velocities. This suggests that a common propagating velocity for the phase shifting of the physical parameters used in the flow rig experiments to derive instantaneous turbine efficiency might not be sufficient. The measurements also showed that a substantial mass accumulation within the turbine occur. Mass storage together with density variations due to pressure and temperature fluctuations led to the conclusion that there is energy storage within the turbine and that a traditional isentropic efficiency can not be derived. This implies that the unsteady turbine performance departs from a quasi-steady turbine performance description.

In recent days Szymko (2006) and Rajoo (2007) used the sum of the bulk and sonic flow velocity for deriving the instantaneous efficiency for mixed-flow turbines on a pulsating flow rig due to that it gave a good correlation between the pressures measured at different locations of the turbine. However, Rajoo

(2007) questions the evaluation of the turbine performance via instantaneous efficiency due to the need of phase shifting.

As a complement to the measurements performed by Dale & Watson (1986), Yeo & Baines (1990) measured the full velocity vector at the rotor inlet with a L2F velocimeter, from which the flow angle and incidence angle was derived. They showed that there are large changes in the velocity and flow angle during the course of an inlet pulse which causes wide variations of rotor incidence angle. Baines & Yeo (1991) showed that the flow variations measured under unsteady flow at the rotor inlet were similar to those measured under steady flow (for partial admission conditions, measurements performed on a twin-entry turbine) and that no unsteady effects could be seen at the rotor exit. The conclusion was that large scale energy transfer in the rotor eliminates unsteady flow effects which implies that the rotor can be seen as a quasi-steady flow device, which implies that the dynamic unsteady effects occur in the volume upstream the rotor. This was at the time contradicted by Winterbone & Alexander (1990) and Winterbone et al. (1991) who measured the pressure at the rotor inlet at different azimuth angles with static pressure taps on the volute wall. They concluded that the dynamic effects in a turbine must come from the rotor due to that the pressures at the rotor inlet for unsteady flow showed similar behaviour as for steady flow.

Lam et al. (2002) performed a computational study on the instantaneous performance of an entire turbine stage for unsteady flow conditions within a 3-dimensional computational fluid dynamic code. Instantaneous turbine efficiency was derived for the entire stage and for the rotor solely. The results showed that the rotor acts as a quasi-steady device when extracting power from the fluid, but when looking at the entire stage there are significant deviations from the quasi-steady behaviour. This implies that the volute influences the unsteady flow conditions seen by the rotor. The results also confirmed the findings of Ehrlich (1998) that flow velocity, pressure and temperature within the volume of the exhaust manifold and turbine propagates with different velocities, i.e. there are both acoustic and convective phenomena.

Lujan et al. (2001) tried a somewhat different approach to derive the on-engine turbine efficiency. Instead of measuring all the thermodynamic properties they used a calibrated 1D gas-dynamic engine model to extract some of the parameters in order to derive the turbine efficiency. They calculated a cycle-average turbine efficiency which was 75% of the efficiency corresponding to the values from the turbine manufacturer measured under steady flow, the measurements did not include turbocharger speed fluctuations.

Westin (2005) used similar approach to determine the thermodynamic properties to calculate the on-engine turbine efficiency. Different approaches to derive the isentropic turbine power were tried to determine the most accurate way to derive instantaneous turbine efficiency on the engine. The most accurate approach chosen was to assume that no mass accumulation within the volume of the turbine occur due to difficulties in measuring/simulating mass accumulation. The volume of the turbine was simply modelled as a straight pipe which gave a noisy and unrealistic isentropic power trace when mass accumulation in the volume was considered. The efficiency calculations did not include any phase shift between measured thermodynamic properties upstream and downstream the turbine and the turbocharger shaft acceleration since no significant phase difference could be seen.

Rehnberg et al. (2006) performed similar instantaneous turbine efficiency calculations as Westin (2005) to show discrepancies between the on-engine instantaneous efficiency calculations and instantaneous efficiencies obtained from measured turbine performance data under steady-flow conditions used with the assumption that the turbine behaves in a quasi-steady manner. The results showed that the efficiency for an exhaust pulse are well matched at the up slope of the pulse until maximum isentropic power and then deviates rapidly as the power from the pulse decreases.

3.2. Twin-entry turbine performance at equal and unequal admission

On multi-cylinder engines twin-entry turbines are used to improve transient response and lower the engine back pressure at exhaust valve opening due to less pulse interference from different cylinders. Several researchers have been measuring the twin-entry turbine performance with different degrees of unequal admission conditions in flow rigs.

Dale & Watson (1986) showed that the mass flow characteristics for each branch of a symmetrical twin-entry turbine at equal pressure ratios is half of the combined flow. However, at unequal admission they concluded that the mass flow characteristics for each branch can not be accurately represented by halving the total flow at equal admission and applying the results to each branch in isolation of the other since the flow in each branch is affected by the pressure ratio in the other branch. They also showed that the efficiency differs with different unequal admission conditions, +5 to -12% from the steady equal admission line as shown in figure 3.2. Capobianco & Gambarotta (1993) performed similar measurements that supported the findings even though their measurements were performed on a twin-entry turbine with asymmetrical volute limbs.

Yeo & Baines (1990) extended the measurements performed by Dale & Watson (1986) with measurements of the full velocity vector from which the flow angle and incidence angle were derived. The measurements showed large variations in incidence angle even at close to design point operation for unequal admission conditions, which affects the turbine performance. Unequal admission conditions were further investigated by Baines & Yeo (1991) who

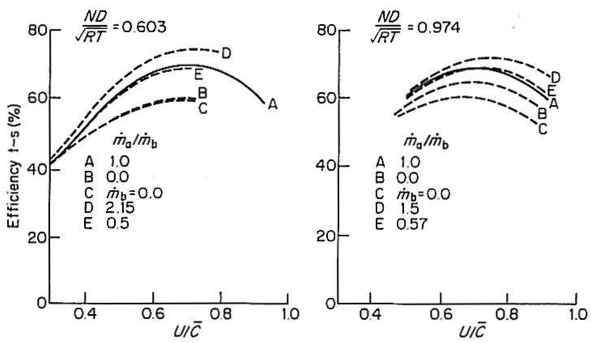

FIGURE 3.2. Efficiency characteristics with unequal admission at two different speeds, Dale & Watson (1986)

showed that at equal admission the incidence angle is close to -30^o at different turbine operating points, but differ substantially for different unequal admission conditions, $\pm 15^o$ for modest degrees of unequal admission (mass flow rate ratio of 0.6 to 2.0) and up to -60^o to $+30^o$ for extreme unequal admission conditions. At these extreme conditions the flow angle was measured to be greater than 90^o near the walls, which implies that recirculation to the other volute limb occurs. The measurements support the 3D simulation results by Lymberopoulos et al. (1988) of the flow within a twin-entry volute.

The measurements performed by Ehrlich (1998) on an engine showed that the turbine works under unequal admission conditions, at high loads as high mass flow ratios as 2.8 to several short periods of extreme unequal admission conditions with zero flow in one of the volute limbs.

Recently, Björnsson et al. (2005) compared the twin-entry turbine performance with a standard design and a lengthened dividing wall versus a single-entry turbine and a parallel turbocharger system via simulations for a 6-cylinder SI engine. The results showed that a twin-entry turbine gives far better transient response and low end torque than a single-entry turbine, similar as to a twin parallel turbo arrangement despite lower efficiency due to unequal admission. This was further improved with a lengthened dividing wall due to a higher overall pulse energy which could be converted into a higher boost pressure.

The twin-entry turbine was modelled with an extended turbine map where the mass flow characteristics were measured at different pressure ratios between the two turbine inlets. An additional flow coefficient was used to increase the flow area of the manifold with the higher pressure and to decrease the flow area of the manifold with the lower pressure within the model. The turbine efficiency was also modelled to be influenced by the added flow coefficient. It was claimed that no connecting pipe between the inlet pipes to the turbine model was needed to model cross flows. Unfortunately, the results were not verified with measured data to show to which extent the pressure traces before the turbine were modelled correctly.

3.3. Modelling turbine performance for pulsating flow

This part will consider turbine models made for the intention to be used within engine simulations. This means that full 3D turbine models will not be considered. Even though these models have proven to give good results they are not suited for engine simulations due to the CPU-time required.

One of the first attempts to model the performance of a vaneless radial turbine under unsteady flow conditions was conducted by Chen & Winterbone (1990). The volute was divided into three stages were the second stage, after the volute tongue as modelled as a tapered pipe with dynamic effects accounted for. All the fluid did continuously move to a third stage where it finally entered the rotor, which was treated as a quasi-steady flow device. The results were unfortunately not verified with measured data under pulsating flow conditions. Chen et al. (1996) improved the model with respect to loss modelling and validated the model with experimental flow data for a mixed-flow turbine under pulsating flow conditions after calibration with measurements for steady flow. The results showed that the unsteady model is better capable of predicting the turbine flow behaviour than a quasi-steady model even though a model which accounts for the circumferential flow variations at the rotor inlet may be necessary.

Circumferential flow variations were considered by Hu (2000) who developed a complete turbine model for a vaneless radial twin-entry turbine to account for dynamic effects such as fluid and mechanical inertia in a pulsating flow. The model was based on the solution of the governing equations of fluid motion for the various turbine components in 1D. For the rotor two control volumes, a radial and an axial were employed to derive the governing equations. An assumption of constant rotor inlet absolute flow angle was made, which was modelled as if there was a vaned diffuser set to the assumed constant flow angle to justify the assumption of 1D flow since otherwise a 2D calculation was claimed necessary. Source terms were used to account for losses which were calibrated from steady flow measurements. The model was validated with experimental data from Ehrlich (1998). Results showed that the model captures the main features of the turbine behaviour under pulsating flow conditions. The model was later refined by King (2002) who performed a more thorough comparison with experimental data and managed to use the turbine model within the 1D engine simulation code GT-Power.

CHAPTER 4

Research Methods

4.1. Experimental method

In the experimental part in paper 1 and paper 2 a standard Scania DC1201 in EuroIII configuration was used. For paper 3 the engine was rebuilt with a two-stage turbocharger system in series and a high pressure loop for EGR. To achieve rapid transient response the high pressure turbine was equipped with a twin-entry volute to prevent exhaust pulses from different cylinders to interfere and a VGT at the low pressure stage for controllability of the gas exchange process.

The data acquisition and test bed control system used for the measurements of engine performance parameters are developed in-house by Professor Hans-Erik Ångström. The data acquisition system enables both high and low frequency signal measurements and can be correlated to the rotation of the crank-shaft with high accuracy. Engine performance parameters were measured as cycle averaged or on a crank-angle resolved basis.

For pressure measurements steel diaphragm gauge pressure transducers from GEMS and Kistler with a range from 1 to 10 bars were used. The sensors at positions where the gas temperature reaches above 150^oC were mounted via water-cooled adapters. Static calibration of the pressure transducers were accomplished by a calibrated pressure indicator with a hand pump from Druck. The transducers were calibrated with an error below 0.5% and 0.08% full scale for the transducers from GEMS and Kistler respectively.

Gas temperatures were measured with shielded 0.5 to 3 mm K-type thermocouples from Pentronic. According to the general assumption this kind of thermocouples, are relatively slow due to their thermal inertia and measures therefore some kind of a time-averaged temperature. However, Westin (2005) compared measured and simulated gas temperatures and found that a 3mm thermocouple with 100mm insertion length measures a temperature close to the mass-averaged temperature. The accuracy of class 1 K-type thermocouples is the larger of 1.5^o and 0.004 times the measured temperature.

Inlet air mass flow rate was measured with a Hot-film meter, Bosch HFM5 mounted in a pipe with a larger area compared to the pipe used by the manufacturer to extend the measurement range. Calibration at AVL in Jordbro showed an error below 1% according to the manufacturer's specifications after scaling with the larger pipe area.

A piezo electric water cooled pressure transducer from AVL was used for the cylinder pressure measurements, which was mounted at one of the 6 cylinders, cylinder 6. A dead weight scale from Ametek was used for the cylinder pressure transducer calibration. The linearity error was found to be within 0.5%.

Turbocharger speeds were measured by measuring and storing the times of the blade passages according to a clock with a counting frequency of 10MHz. The blade passages were detected with an eddy-current probe from Micro-Epsilon mounted in the compressor housing.

The EGR rate in paper 3 was measured via the ratio of carbon dioxide, CO_2 level added to the amount of fresh air in the intake and the exhaust manifold. This was accomplished with two non-dispersive infra red light analyzers from Maihak, Boo-Instruments.

4.2. Turbocharger Modelling

A standard approach to derive turbocharger performance within engine simulation codes is to include turbine and compressor performance data in the form of lookup tables directly into the engine model, Gamma Technologies (2004) and Rakopoulos & Giakoumis (2006). These models are based on steady-flow rig measurement of the turbine and compressor used under the assumption that the flow within the turbomachine is quasi-steady, i.e. behaves at any instant in time as under steady flow conditions. The turbocharger manufacturers specify the performance characteristics in terms of mass flow rate and efficiency versus rotational speed and pressure ratio. Computational fluid dynamics based engine simulation codes then use the turbine and compressor sub-models to evaluate the mass flow rate and efficiency outputs for a given rotor speed and pressure ratio at every time step during the simulation.

The turbine and compressor performance parameters needed to define steady operation of the turbomachine are usually specified as quasi-nondimensional parameters to take the inlet conditions into account. For the turbine, i.e. reduced speed (N_{red}), reduced mass flow ($\dot{m}_{red}$) and pressure ratio (PR) as,

$$N_{red} = \frac{N}{\sqrt{T_0}} \tag{4.1}$$

$$\dot{m}_{red} = \frac{\dot{m}\sqrt{T_0}}{P_0} \tag{4.2}$$

$$PR = \frac{P_{0,in}}{P_{exit}} \tag{4.3}$$

where (P_0) denotes inlet pressure and (T_0) inlet temperature. An example of a turbine map is shown in figure 4.1. The compressor performance data is usually presented with corrected parameters where the inlet temperature and pressure in the reduced expressions are scaled with a reference temperature and pressure respectively.

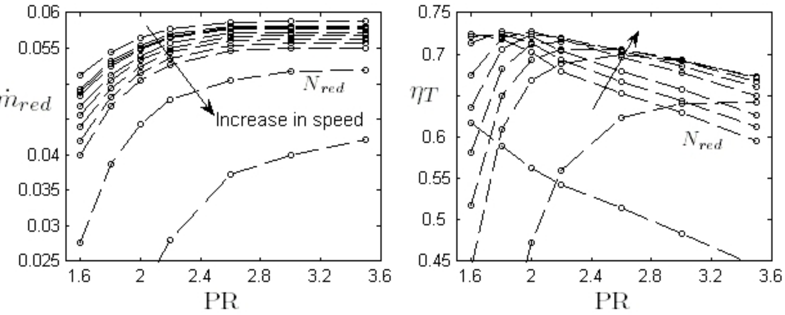

FIGURE 4.1. Measured flow characteristics and efficiency for a radial turbine on a steady-flow rig. Each line corresponding to a constant speed, data from Paper 2.

The power produced/consumed by the turbine/compressor are derived from the Euler equation, equation 2.3 via the isentropic relation including losses,

$$P_T = \eta_T \dot{m} c_p T_{0,in} \left(1 - \left(\frac{p_{0,out}}{p_{0,in}} \right)^{\gamma - 1/\gamma} \right) \tag{4.4}$$

$$-P_C = \frac{1}{\eta_C} \dot{m} c_p T_{0,in} \left(1 - \left(\frac{p_{0,out}}{p_{0,in}} \right)^{\gamma - 1/\gamma} \right) \tag{4.5}$$

The pressure ratios are calculated from the adjacent volumes of the turbine/compressor. The turbocharger speed is derived from the torque imbalance associated with the compressor and turbine power between the turbine, compressor and frictional losses in the shaft assembly according to,

$$\frac{d\omega_{TC}}{dt} = \frac{\eta_{mech} P_T - P_C}{I} \tag{4.6}$$

To model a twin-entry turbine with the software GT-Power the solver uses two turbine objects based on a single volute turbine map since the turbine performance data is usually measured at equal admission. By default the mass flow to each turbine or turbine inlet is divided evenly between the two. To reproduce the pressure trace upstream the twin-entry turbine an orifice connection is usually applied between the two inlet pipes to the turbine volute to allow for cross flows or leakages within the turbine. Unfortunately, there does not exist any good way to find the area of the orifice connection based on the turbine volute geometry. From communications with Gamma Technologies.

CHAPTER 5

Results

The work described in **Paper 1** shows the on-engine twin-entry turbine behaviour from derived instantaneous turbine efficiency calculations. The instantaneous turbine efficiency was derived according to Winterbone & Pearson (1998) from measured and simulated data. Phase differences between measured/simulated isentropic conditions upstream the turbine and the turbocharger shaft acceleration was not considered, which, as shown in the literature survey in chapter 3, can have a significant affect on the results. However, the results showed that there is a significant asymmetry in the on-engine twin-entry turbine performance as shown in figure 5.1, which could not be captured by a straight forward simulation. A higher efficiency was obtained for exhausts from the cylinders that are connected to the outer volute entry even though the twin-entry volute is symmetric, according to the measurements by Dale & Watson (1986). Differences in turbine efficiency were also shown for exhausts from cylinders with different exhaust manifold lengths where a longer exhaust manifold gave higher turbine efficiency than cylinders with a shorter exhaust manifold.

The possibilities to generate turbine performance data with the software, Rital by Concepts NREC (2005) and how it performs for engine simulation compared to directly measured turbine performance data are shown in **paper 2**. The turbine design software was used to model the turbine and generate a full resolution turbine map for a twin-entry turbine, but without the direct possibility to model the twin-entry volute. The model was calibrated with turbine performance data from the turbine manufacturer measured with a steady-flow flow rig at equal admission conditions. Figure 5.2 shows the full resolution turbine map including measured data from the turbine manufacturer and a turbine operation trace from the full engine simulation for the second engine cycle after the start of the transient. The measured turbine performance data from the turbine manufacturer was extrapolated with GT-Power's own extrapolation routine to obtain a full resolution map necessary for engine simulations.

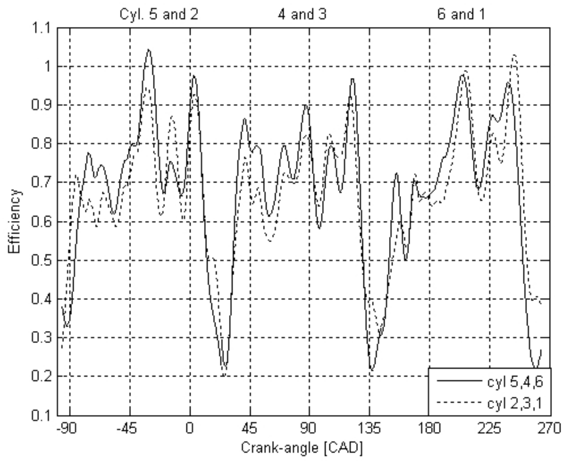

FIGURE 5.1. Efficiency comparison for the two cylinder banks overlaid. Numbering of the blowdown phasing from different cylinders are shown above in the figure, from Paper 1.

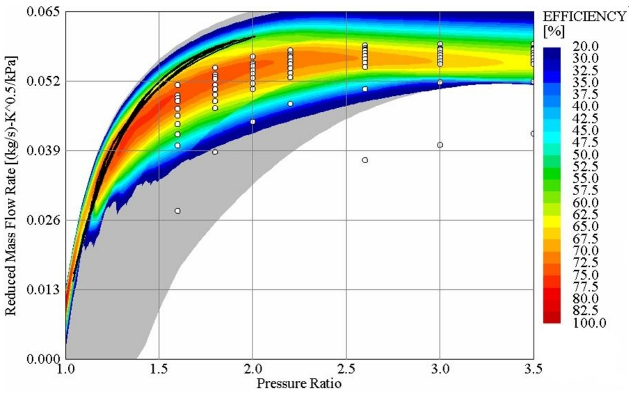

FIGURE 5.2. Full resolution turbine map generated with Rital including turbine performance data from the turbine manufacturer, white dots. The black lines at the edge of the map shows turbine operation for a cycle at the start of the load transient simulated, from Paper 2.

The results from the engine simulation during the load transient at constant speed showed that the two differently obtained turbine maps behave similarly when incorporated into the engine model. To obtain similar turbocharger speed in the simulation as in the measurements during the load transient studied the turbine efficiency multiplier was raised by 30%. Results from the literature, see e.g. Dale (1990) shows that the turbine efficiency is lower and not higher under pulsating flow conditions, but on the other hand the energy content in a pulse pressure wave contains more isentropic specific work than a steady flow one with the same cycle mean pressure ratio. However, incorrect simulated exhaust gas energy content can be compensated for with a raised turbine efficiency multiplier. Unfortunately, the actual exhaust gas energy content on the engine was not measured due to difficulties in measuring the temperature and mass flow rate in the exhaust manifold fast enough.

The study presented in **paper 3** shows to which extent it is possible to simulate the performance of a diesel engine with a complex gas-exchange system including two-stage turbocharging and short route EGR in transient operation, i.e. during a load transient. The turbocharging arrangement included a twin-entry turbine at the high pressure stage for rapid transient response and VGT at the low pressure stage for controllability of the gas exchange system. The results show that it is difficult to fully predict turbine performance since the turbine performances had to be manipulated with up to 10% to capture the measured engine performance, figure 5.3 and 5.4. Dynamic effects from the turbine volume are not considered in the turbine model that was based on steady-flow rig measured turbine performance data. A significant phase difference could be seen when comparing the simulated and measured turbocharger shaft acceleration, especially for the low pressure turbine. The volute had to be modelled since it affects the pressure amplitude upstream the turbine. Here, the turbines volutes were modelled as straight pipes with a volume of 70% of the entire volute volume. Since the volute is not a straight pipe as modelled, the distance for the flow to pass before approaching the rotor will not be modelled correctly, which introduces the phase error.

However, even though the model was not able to perfectly capture the engine performance in detail, it was shown that it is highly usable for concept studies as a help in engine design.

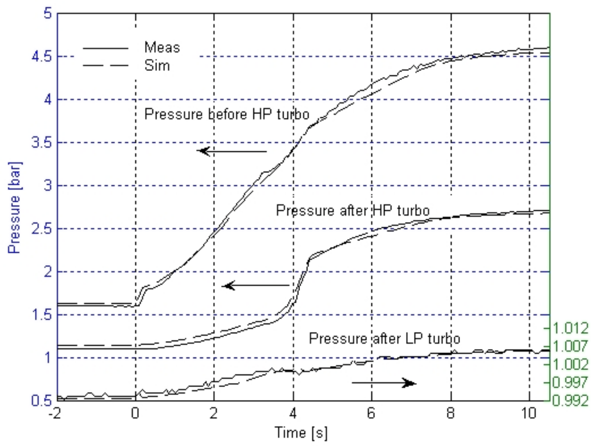

FIGURE 5.3. Mean cycle resolved pressures from the calibrated model before and after the high pressure turbine and after the low pressure turbine. The VGT was held open during the transient and was then closed to obtain 30% EGR at high load, from Paper 3.

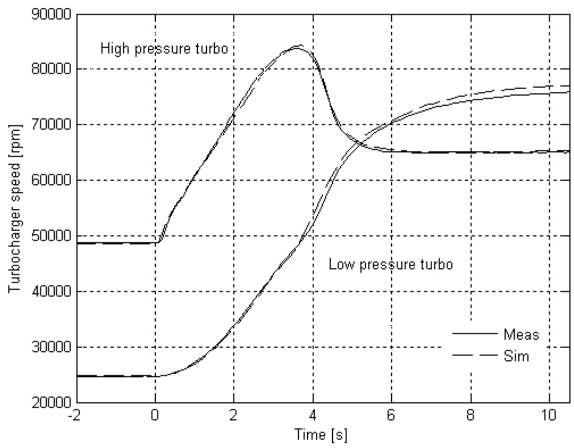

FIGURE 5.4. High and low pressure turbocharger speeds, from Paper 3.

CHAPTER 6

Concluding Remarks

As the review presented in chapter 3 has shown there is a clear discrepancy in turbine performance for steady and pulsating flow conditions. Several researchers have stated that the quasi-steady approach to predict turbine performance for unsteady flow will most likely not be sufficient. The results from Paper 2 and Paper 3 show that the attempts to accurately predict on-engine turbine performance for transient engine operation have not been successful. When trying to predict turbine performance with steady-flow rig turbine performance data the difficulties added compared to stationary operation are long scale transients as wall temperature gradients in the cylinder and the exhaust manifold which directly influences the isentropic energy to the turbine. This makes it even more difficult to predict the isentropic exhaust gas energy content compared to for stationary operation and to estimate how well the turbine model actually performs.

Several problems arise when using turbine performance data in the form of look-up tables to model the turbine within simulations for reciprocating internal combustion engines,

1. The turbine maps are used under the assumption that the turbine works under quasi-steady conditions.
2. Performance data for low powers are usually not measured by the turbo manufacturer due to difficulties in obtaining data with high accuracy in this area and therefore have to be extrapolated. This is especially important for low load operation.
3. The turbocharger sub-model based on turbine performance data does not consider the volume of the volute, thus no dynamic effects from the volute volume are considered within the sub-model.
4. Performance data for turbines equipped with a twin-entry volute are usually measured under equal admission which gives erroneous performance data for partial admission conditions.

Another drawback when using measured turbine performance data as a base for the turbine model is that there is no possibility to change any internal turbine parameters without designing and producing a new turbine with the wanted design and to measure its characteristics. Today, the only possibility to change the behaviour of the actual turbine is to scale the in advance measured data set, which limits the possibilities to try different designs.

In order to avoid these problems and to be able to perform more predictive simulations it would be necessary to have a physical turbine model based on its geometry which considers dynamic effects. Such a model would also allow internal turbine parameter changes.

6.1. Future work

The turbine model presented by Hu (2000) and King (2002), which include dynamic effects under unsteady flows seems as the most promising step taken to improve the turbine model for full engine simulations with respect to CPU time and accuracy. The model was based on the solution of the governing equations of fluid motion for the various turbine components in 1D. To solve the governing equations in only 1D, the vaneless turbine was modelled as a turbine with a vaned diffuser with the assumption that the inlet flow angle to the rotor is constant. As most turbines for automotive applications are vaneless the aim is to extend the model to yield for non-constant rotor inlet flow angles. If this is possible with a 1D approach or if a 2D approach is necessary as claimed by the authors has to be investigated. To account for losses the model used by Rital would be possible to use for model calibration under steady-flow conditions since it gives losses for the various turbine stages and not only the complete stage performance.

Acknowledgements

First, I would like to thank my always so enthusiastic supervisor Professor Hans-Erik Ångström for giving me the opportunity to work on this project and for the guidance throughout the work.

Roger Olsson and Ylva Björklund at the gas exchange group, Scania CV for technical support.

Per Risberg for all the help when it comes to proof reading.

This work is financed by the Swedish National Energy Administration - STEM which is greatly appreciated.

Scania CV is appreciated for the material support.

and to all you former and present colleagues for all the interesting discussions and the encouragement.

March 2008, Stockholm
Niklas Winkler

References

ARCOUMANIS C., KARAMANIS N. MARTINEZ-BOTAS R.F., SU C.C. 1999 Unsteady characteristics of a mixed-flow turbocharger turbine *3rd European Conference on Turbomachinery-(London), 1999, Pages: 905 - 922, C557/30/99*

BAINES N. C. & YEO J. H. 1990 Pulsating flow behaviour in a twin-entry vaneless radial-inflow turbine *IMechE Paper no. C405/004/90*

BAINES N. C. & YEO J. H. 1991 Flow in a radial turbine under equal and partial admission conditions *IMechE Paper no. C423/002/91*

BAINES N. C., HAJILOUY-BENISI A. & YEO J. H. 1994 The pulse flow performance and modelling of radial inflow turbines *IMechE Paper no. C484/006/94*

BAINES N. C. 2003 Axial and Radial Turbines, Radial Turbine Design *Concepts NREC, ISBN 0-933283-12-0*

BAINES N. C. 2005 Fundamentals of Turbocharging *Concepts NREC, Wilder, VT, ISBN 0-933283-14-8*

BJÖRNSSON H., OTTOSSON A., RYDQUIST J.-E., SPADER U. & SCHORN N. 2005 Optimizing the SI-engine turbo systems for maximum transient response. Methods, factors and findings *10 Aufladetechnische Konferenz, Dresden, Paper No. 22*

CAPOBIANCO M., GAMBAROTTA A, & CIPOLLA G. 1989 Influence of the pulsating flow operation on the turbine characteristics of a small internal combustion engine turbocharger. *IMechE Paper no. C372/019*

CAPOBIANCO M. & GAMBAROTTA A. 1993 Performance of a twin-entry automotive turbocharger turbine *ASME Energy-Sources Technology Conference & Exhibition, Paper No. 93-ICE-2*

EASY! FOR TURBINES TUTORIAL April 2005 version 7.7.70 *Concepts NREC*

CHEN H. & WINTERBONE D. E. 1990 A method to predict performance of vaneless radial turbines under steady and unsteady flow conditions *IMechE Paper no. C405/008*

CHEN H., HAKEEM I. & MARTINEZ-BOTAS R. F. 1996 Modelling of a turbocharger turbine under pulsating inlet conditions *IMechE Proc Instn Mech Engrs, pp 397-408*

DALE A. & WATSON N. 1986 Vaneless radial turbocharger turbine performance *IMechE Paper no. C110/86*

DALE A.P. 1990 Radial, Vaneless Turbocharger Turbine Performance *Doctoral Thesis, Imperial College, London*

EHRLICH D. A. 1998 Characterization of unsteady on-engine turbocharger turbine performance *Doctoral Thesis, Purdue University*

GT-POWER User's Manual, version 6.1 *Gamma Technologies 2004*

HEIZLER H. 1995 Advanced Engine Technology *SAE ISBN 1-56091-734-2*

HU X. 2000 An advanced turbocharger model for the internal combustion engine *Doctoral Thesis, Purdue University*

JAPIKSE D. AND BAINES N. C. 1997 Introduction to turbomachinery *Concepts ETI, Inc. and Oxford University Press, ISBN 0-933283-10-5*

KING A. J. 2002 A turbocharger unsteady performance model for the GT-Power internal combustion engine simulation *Doctoral Thesis, Purdue University*

LAM J.K-W., ROBERTS Q.D.H. & MCDONNEL G.T. 2002 Flow modelling of a turbocharger turbine under pulsating flow *IMechE Paper no. C602/025/2002*

JOSE P. LAGUNA-GOMEZ EU Legislative Perspective 2007. *Heavy-Duty Emissions Control Symposium, Gothenburg 2007.*

LUJAN J.M., GALINDO J. & SERRANO J.R. 2001 Efficiency characterization of centripetal turbines under pulsating flow Conditions *SAE Paper no. 2001-01-0272*

LYMBEROPOULOS N., BAINES N. C. & WATSON N. 1988 Flow in Single and Twin-Entry Radial Turbine Volutes *ASME Paper No. 88-GT-59*

RAJOO S. 2007 Steady and Pulsating Performance of a Variable Geometry Mixed Flow Turbocharger Turbine *Doctoral Thesis, Imperial College, London*

RAKOPOULOS C. D. & GIAKOUMIS E. G. 2006 Review of Thermodynamic Diesel Engine Simulations under Transient Operating Conditions *SAE Paper no. 2006-01-0884*

REHNBERG U., ANGSTROM H-E. & OLOFSSON U. 2006 Instantaneous On-Engine Turbine Efficiency for an SI engine in the closed waste gate region for 2 different turbochargers *SAE Paper no. 2006-01-3389*

SZYMKO S. 2006 The development of an Eddy Current Dynamometer for Evaluation of Steady and Pulsating Turbocharger Turbine Performance *Doctoral Thesis, Imperial College, London*

WALLACE F. J. & BLAIR G. P. 1965 The pulsating-flow performance of inward radial-flow turbines 65-gtp-21 *ASME, p. 1-19 1965*

WATSON N. & JANOTA M. S. 1982 Turbocharging the internal combustion engine *MacMillan Press ISBN 0-933283-10-5*

WESTIN F. 2005 Simulation of turbocharged SI-engines - with focus on the turbine *Doctoral Thesis, Royal Institute of Technology - KTH, Stockholm*

WINTERBONE D. E. & ALEXANDER G. I. 1990 Measurements of the performance of a radial inflow turbine in conditional steady and unsteady flow *IMechE paper no. C405/015*

WINTERBONE D. E., NIKPOUR B. & FROST H. 1991 A contribution to the understanding of turbocharger turbine performance in pulsating flow *IMechE Paper no. C433/011*

WINTERBONE, D. E. & PEARSON, R. J. 1998 Turbocharger turbine performance under unsteady flow - a review of experimental results and proposed models *IMechE Paper no. C554/031/98*

YEO J. H. & BAINES N. C. 1990 Pulsating flow behaviour in a twin-entry vaneless radial-inflow turbine *IMechE Paper no. C405/004/90*

WWW.AMETEKCALIBRATION.COM

www.AVL.com

www.boo-instrument.se

www.bosch.com

WWW.DRUCK.COM

WWW.GEMSSENSORS.COM

WWW.KISTLER.COM

WWW.MICRO-EPSILON.DE

WWW.PENTRONICH.SE